European Journal of Nuclear Medicine and Molecular Imaging (2021) 48:204–216
https://doi.org/10.1007/s00259-020-04915-7

ORIGINAL ARTICLE

Theranostic implications of molecular imaging phenotype of well-differentiated pulmonary carcinoid based on ^{68}Ga-DOTATATE PET/CT and ^{18}F-FDG PET/CT

Lamiaa Zidan[1,2] · Amir Iravani[1,3] · Grace Kong[1,3] · Tim Akhurst[1,3] · Michael Michael[3,4] · Rodney J Hicks[1,3]

Received: 28 February 2020 / Accepted: 7 June 2020 / Published online: 22 June 2020

Abstract

Purpose This study aimed to analyse the molecular imaging (MI) phenotype of typical carcinoid (TC) and atypical carcinoid (AC) by ^{68}Ga-DOTATATE (GaTATE) and ^{18}F-FDG (FDG) PET/CT with the emphasis on its potential theranostic implications for peptide receptor radionuclide therapy (PRRT).

Methods Retrospective review of patients with biopsy-proven TC or AC undergoing both GaTATE and FDG PET/CT at presentation. Based on correlative CT or MRI, positive lesions on either scan were defined by uptake above liver parenchyma. Per patient MI phenotypic pattern was classified as score 1, if all lesions were negative on both scans; score 2, if all were GaTATE positive/FDG negative; score 3, if all lesions were GaTATE positive but some or all were also FDG positive and score 4, if there were any GaTATE negative/FDG positive lesions. Scores 1 and 4 were deemed unsuitable for PRRT.

Results Of 56 patients (median age 66.5 years, 32 female), 22 had TC, and 34 had AC. Distant metastases were seen in 32% of TC and 94% of AC. At a median follow-up of 37 months for TC and 38 months for AC, 100% and 63% were alive, respectively. Median OS for AC was 56 months (95% CI 43, not reached [NR]), and TC was NR. On inter-patient dual-tracer analysis, scores 1, 2, 3 and 4 were 23%, 18%, 36% and 23% in TC and 3%, 15%, 32% and 50% in AC, respectively. In 16 patients (score 2, $N = 3$; score 3, $N = 12$; score 4, $N = 1$) who were treated with PRRT, disease control rate at 3 months and OS were, 85% and 54.6 months (95% CI 44–70), respectively.

Conclusions TC and AC showed a wide inter-patient phenotypic heterogeneity on GaTATE and FDG with around half of patients (46% TC and 53% AC) having an unsuitable phenotype for PRRT. Dual-tracer MI phenotype can be used to select the most suitable patients for PRRT.

Keywords Pulmonary carcinoid · ^{68}Ga-DOTATATE PET/CT · ^{18}F-FDG PET/CT · Peptide receptor radionuclide therapy

This article is part of the Topical Collection on Oncology - Chest

Lamiaa Zidan and Amir Iravani are co-first authors

Electronic supplementary material The online version of this article (https://doi.org/10.1007/s00259-020-04915-7) contains supplementary material, which is available to authorized users.

✉ Lamiaa Zidan
lamiazidan@gmail.com

Amir Iravani
amir.iravani@wustl.edu

Grace Kong
Grace.Kong@petermac.org

Tim Akhurst
Tim.Akhurst@petermac.org

Michael Michael
Michael.Michael@pertermac.org

Rodney J Hicks
rod.hicks@petermac.org

[1] Cancer imaging, Peter MacCallum Cancer Centre, Melbourne, Victoria, Australia

[2] Clinical Oncology and Nuclear Medicine department, Cairo University, Cairo, Egypt

[3] Sir Peter MacCallum Department of Oncology, The University of Melbourne, Melbourne, Victoria, Australia

[4] Division of Oncology, Peter MacCallum Cancer Centre, Melbourne, Victoria, Australia

Introduction

Pulmonary neuroendocrine neoplasia (NEN) is classified according to the degree of differentiation into well and poorly differentiated subtypes, depending on the mitotic index and the presence of necrosis [1, 2]. The proliferation index by Ki-67 immunostaining is a potential meaningful marker to separate well-differentiated from poorly differentiated NENs. However, it is not included in the current WHO classification criteria [3–5]. The well-differentiated group, also known as pulmonary carcinoid or bronchial neuroendocrine tumour (NET), includes the typical carcinoid (TC), which is considered low-grade and atypical carcinoid (AC), which is of an intermediate-grade. The poorly differentiated group includes large cell neuroendocrine carcinoma (LCNEC) and small cell lung carcinoma (SCLC) [4, 6]. Although there are some similarities between the two groups, the clinical behaviour and prognosis of pulmonary carcinoids is completely different from that of SCLC and LCNEC [7]. They also differ molecularly, with the poorly differentiated tumours, particularly SCLC, characteristically having loss of *p53* and *Rb* [8].

Based on histology, approximately 60 to 80% of pulmonary NEN express somatostatin receptors (SSTR) and may therefore benefit from somatostatin receptor-based imaging [9]. Gallium68-labelled radiopharmaceuticals, including ^{68}Ga-DOTATOC, ^{68}Ga-DOTANOC and ^{68}Ga-DOTATATE PET/CT (GaTATE-PET), have replaced ^{111}In-pentereotide (Octreoscan) because of their higher diagnostic accuracy, shorter scan time and lower radiation dose. GaTATE-PET has a higher affinity for SSTR-2; it provides accurate information about disease sites, burden and SSTR expression [10–13]. A high impact on management has also been demonstrated by our group in the transition to GaTATE-PET [14]. On the other hand, ^{18}F-FDG-PET/CT (FDG-PET) has a complementary role in the characterization of NET, especially those with a high proliferation index (Ki-67), which tend to have high glycolytic metabolism but low or no SSTR expression [15]. Several studies have, however, also demonstrated a variable degree of FDG uptake in well-differentiated pulmonary NET, particularly AC [16, 17]. Molecular imaging (MI) using both GaTATE and FDG-PET allows identification of patients with sites of well-differentiated and poorly-differentiated disease respectively, and it reflects disease heterogeneity on a whole-body basis, overcoming the limitation of histopathology which is usually performed on a single disease site [18].

Peptide receptor radionuclide therapy (PRRT) with radiolabelled SSTR agonists, ^{90}Y-DOTATOC and ^{177}Lu-DOTATATE, has been successfully used to target metastatic and inoperable NET [19]. The application of PRRT is guided by diagnostic MI. Multiple studies have suggested SSTR PET/CT uptake intensity of more than the liver is required to indicate potential suitability of PRRT [20–23]. Patients with FDG positive/SSTR negative imaging phenotype may have sites of aggressive disease that cannot effectively be targeted with PRRT [20]. The importance of using combined GaTATE and FDG-PET has been demonstrated for gastroenteropancreatic (GEP) NET [24]. However, the assessment of pulmonary NET for the suitability of PRRT using dual tracer imaging has yet to be established.

This study aims to assess the heterogeneity of MI phenotype in pulmonary NET by sequential GaTATE and FDG-PET at baseline evaluation and thereby guiding appropriate therapy. We have also correlated the MI phenotype and semi-quantitative uptake parameters with the histopathological subtype and patients' outcome. The outcome of patients who underwent PRRT based on detail molecular imaging characterization is also described.

Materials and methods

This study is a retrospective review of patients with pulmonary NEN extracted from the in-house database picture archiving and communication system (PACS) at Peter MacCallum Cancer Centre during the period from 2006 to 2019, corresponding to the period following introduction of LuTATE PRRT in our department. This study was conducted after receiving the ethical approval of the Peter MacCallum Cancer Centre Ethics Committee (HREC# 19/214R).

Inclusion criteria were met by patients with biopsy-proven, well-differentiated pulmonary NET; TC or AC, with contemporaneous FDG-PET and GaTATE-PET studies at referral, performed within 3 months. Patients with biopsy-proven, poorly differentiated pulmonary NEN, SCLC and LCNEC, were excluded. All pathological reports were reviewed and classified as TC or AC according to the World Health Organization criteria [4].

PET/CT protocol

A PET/CT hybrid system was used, including either Siemens Biograph 64 PET/CT (Siemens Medical Solutions, Erlangen, Germany), GE Discovery 710 PET/CT or GE Discovery 690 PET/CT (GE Healthcare, Milwaukee, WI). For GaTATE-PET, the patients were well hydrated with water without fasting requirements. A dose of 2.6 MBq/kg was slowly injected over 2 min via an IV cannula. Uptake time was a minimum of 45 min before commencing the acquisition of the PET/CT scan. For FDG-PET, a minimum of 6 h fasting and blood glucose level (BGL) less than 11 mmol/L was required before the injection of ^{18}F-FDG. Patients with a BGL > 11 mmol/L were prepared using our published insulin protocol [25]. A dose of 3.5 MBq/kg via an IV cannula was administered, and the patients were rested for at least 60 min before starting the PET/CT scan. PET/CT scan was performed

from vertex to mid-thigh; at first low dose, a non-enhanced CT scan was acquired for attenuation correction using 120 kV (140 kV in extra-large patients), 3.7 mm slice thickness. PET scan was performed after low-dose CT in 3D mode at 2–4 min sequential overlapping bed positions.

Image analysis

The PET/CT studies were reviewed and interpreted by the consensus of two experienced nuclear medicine physicians blinded to the clinical data, using qualitative and semi-quantitative measures using the MIM software (MIM 6.7.11; MIM Software, Cleveland, OH).

Single-tracer analysis

FDG-avidity was graded based on simplified Deauville score scaling with tumour uptake relative to liver uptake as follows: 0, no uptake; 1, above blood pool and less than the liver; 2, equal to the liver; 3, moderately above the liver; 4, markedly above the liver. As the majority of the patients had liver lesions, uptake above the liver background was considered as FDG positive lesion. Therefore, uptake groups 3 or 4 were considered FDG positive, while scores 0–2 (tracer uptake ≤ liver) were negative [26].

^{68}Ga-DOTATATE-avidity was graded based on the modified Krenning scale as follows: 0, no uptake; 1, less than the liver; 2, equal to the liver; 3, above the liver but less than the spleen; 4 equal or more than the spleen or SUVmax > 30 in the absence of a spleen. A GaTATE positive lesion was defined as a tracer uptake group of 3 or 4.

To minimize the potential impact of partial volume artefact, lesions were only considered assessable if more than 1 cm in diameter and of non-cystic appearance. FDG and GaTATE SUVmax of the lesions with the highest avidity were measured. FDG and GaTATE whole-body molecular imaging tumour volume (MITV) were assessed using the whole-body semi-automatically threshold method by the MIM software, for lesions with higher than the liver SUVmean +2 standard deviation (SD) threshold for FDG and lesions with higher than SUVmean liver threshold for GaTATE. Two nuclear medicine physicians agreed on the volumes.

Dual-tracer analysis, inter-patient

A patient-based MI phenotypic score was assigned to each patient as follows: score 1, if all anatomical lesions suggestive of disease were negative on both tracers; score 2, if all lesions were GaTATE positive but FDG negative; score 3, if all lesions were positive on GaTate but some or all were also positive on FDG-avid; and score 4, if some or all were FDG positive but GaTATE negative (spatially discordant disease FDG-avidity). Patient-based dual-tracer scores 2 and 3 were considered suitable to undergo PRRT. The rationale for this categorisation was to mainly guide the suitability of the patients for PRRT based on having the targetable disease (GaTATE positive lesions) and absence of non-targetable disease (spatially discordant FDG-avid lesions).

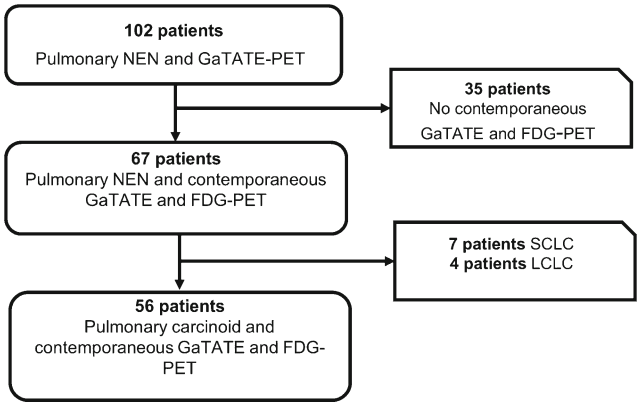

Fig. 1 Consort diagram of the patients

PRRT

The patients must have fulfilled institutional inclusion criteria for PRRT including either documented imaging progression or uncontrolled symptoms on approved medical therapies and adequate hematologic and renal function as previously detailed in prior publications from our group [27, 28]. The treatment regimen typically included four cycles of ^{177}Lu-DOTATATE given 6–10 weeks apart. The patients with bulky tumours > 4 cm were considered for ^{90}Y-

Table 1 Patient characteristics

	TC	AC
Patients	22	34
Age, median (range)	63 (21–81)	68.5 (33–83)
Gender		
Female (%)	13 (59)	19 (56)
Male (%)	9 (41)	15 (44)
Mitotic index, median (range)	0 (0–1)	6 (0*–15)
Necrosis (%)	No necrosis	13 (38)
Ki 67, median (range)	4 (1–16)	14 (5–50)
Prior therapy		
None	16	12
Surgery ± SSA	5	20
Chemotherapy	1	2
Metastatic at MI assessment (%)	7 (32%)	32 (94%)

AC atypical carcinoid, *SSA* somatostatin analogues, TC typical carcinoid

* Pathology showed mitotic index 0 and presence of necrosis in 2 patients and were classified as AC

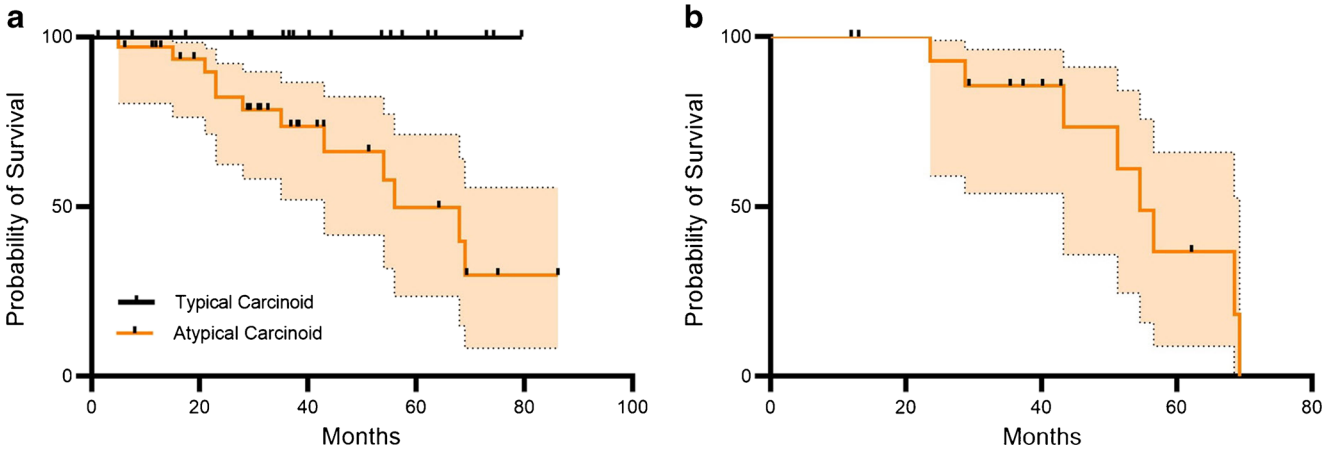

Fig. 2 Kaplan Meier depiction of the overall survival in typical and atypical carcinoid (**a**) and PRRT subgroup (**b**)

DOTATATE for 1–2 cycles (followed by ^{177}Lu-DOTATATE) based on previous experience showing that bulky disease is an adverse prognostic factor for response to ^{177}Lu-DOTATATE PRRT [27, 29]. Each cycle of PRRT was administered with premedication antiemetic and renoprotective amino-acid infusion. The 2nd to 4th cycles of ^{177}Lu-DOTATATE were usually given with radiosensitising chemotherapy, unless contraindicated [28, 30]. Response assessment at 3 months post-PRRT was performed by CT and defined by Response Evaluation Criteria in Solid Tumours (RECIST 1.1) [31] as complete response (CR), partial response (PR), stable disease (SD) or progressive disease (PD).

Statistical analysis

The patients' characteristics and MI parameters are summarized using the median (interquartile range [IQR] and/or range) or basic proportions for continuous and categorical variables, respectively. Overall survival was recorded as the duration from the initial MI assessment to last follow-up or death. The cut-off follow-up date was 1st of October 2019. Fisher's exact test was used to compare the proportion of patients with different dual-tracer MI phenotypes. Mann–Whitney test was used for comparison of non-parametric continuous variables. The median overall survival (OS) was estimated in AC and TC and demonstrated by Kaplan–Meier curves. Due to the absence of any event in TC, correlation with OS is only made in the AC cohort. The MI parameters were divided by the median and correlated with OS using log-rank test only in the AC group.

Results

Fifty-six patients with pulmonary NET met the inclusion criteria (Fig. 1), with median age, 66.5 years; range, 21–83 and 32 females. The median interval time between the histopathology and MI studies was 2 months (range 0–59, IQR 0.6–4.7 months). Twenty-two patients had TC (mitotic index range 0–1, no necrosis and Ki67 range 1–16%), and 34 patients had AC (mitotic index range 0–15, 38% had necrosis, Ki67 range 5–50%) (Table 1). There were two patients with scanty mitotic index but the presence of necrosis on histopathology, hence classified as AC. Seventy-three percent of TC patients and 35% of AC patients had not received any treatment before MI assessment (Table 1). Metastatic disease was more common in AC patients compared with TC patients, $p < 0.0001$. At a median follow-up of 37 months, all TC patients were alive. At a median follow-up of 38 months for AC patients, 21/34 (62%) were alive, and one patient was lost to follow-up. The median overall survival (OS) for AC patients was estimated at 56 months (95% CI 43, not reached) (Fig. 2).

Table 2 Single-tracer analysis

^{68}Ga-DOTATATE intensity score (modified Krenning score)		
	TC	AC
0	3 (14%)	1(3%)
1	6 (27%)	17 (50%)
2	–	–
3	3 (14%)	6 (18%)
4	10 (45%)	10 (29%)
^{18}F-FDG intensity score		
0	3 (14%)	4 (12%)
1	6 (27%)	1 (3%)
2	–	1 (3%)
3	13 (59%)	23 (67%)
4	–	5 (15%)

Table 3 Semi-quantitative analysis of ^{68}Ga-DOTATATE and ^{18}F-FDG PET/CT

Median	TC	AC	*p*
^{68}Ga-DOTATATE SUVmax	14.9 (range 1–70)	8.2 (range 1.6–99)	0.3
OS by median SUVmax		< 8.2 vs ≥ 8.2	0.6
^{18}F-FDG SUVmax	3.7 (range 1.2–13.3)	6.3 (range 1.6–29)	0.02*
OS by median SUVmax		< 6.3 vs ≥ 6.3	0.4
^{68}Ga-DOTATATE MITV	19 (range 1–1500)	51 (range 1–3333)	0.2
OS by median MITV (mL)		< 51 vs ≥ 51	0.2
^{18}F-FDG MITV	20 (range 1–600)	53.5 (range 1–3200)	0.3
OS by median MITV (mL)		< 53 vs ≥ 53	0.1

MITV molecular imaging tumour volume

*Statistically significant

Single-tracer analysis

In TC, 13/22 (59%) patients had at least one GaTATE positive lesion with the majority (10/13 [77%]) of high avidity (modified Krenning score 4), but 41% did not have any GaTATE positive lesions. While a similar proportion of patients (13/22 [59%]) were FDG positive, the intensity of uptake was generally moderate (intensity score of 3) (Table 2).

In AC, 16/34 (47%) patients had at least one GaTATE positive lesion, two-thirds (10/16 [63%]) of modified Krenning score 4, but approximately half (53%) lacked any positive lesions. The majority of patients (28/34 [82%]) were FDG positive but also of moderate avidity (intensity FDG score of 3) (Table 2).

Table 3 details the MI parameters of both tracers in TC and AC. Although FDG SUVmax in AC was significantly higher than TC ($p = 0.02$), no significant difference was found between GaTATE SUVmax of TC and AC ($p = 0.3$) (Supplementary Fig). No significant correlation was found between MI parameters and OS in AC patients (Table 3).

Dual-tracer analysis, inter-patient

The median time interval between the GaTATE-PET and FDG-PET was 10 days (range 0–90 days), with no treatment in-between the scans. On inter-patient dual-tracer analysis, scores 1, 2, 3 and 4 were 23%, 18%, 36% and 23% in TC and 3%, 15%, 32% and 50% in AC, respectively (Table 4, Figs. 3, 4, 5 and 6). On dual-tracer analysis, while the proportion of patients GaTATE negative/FDG negative (score 1) was more common in TC (23% in TC vs. 3% in AC, p 0.03), the distribution of other MI phenotypes (scores 2, 3 and 4) was not statistically significant (Supplementary Fig. 1). Overall, 54% of patients with TC and 47% of patients with AC had a suitable MI phenotype for PRRT (Table 4).

Dual-tracer analysis, intra-patient

A third of all patients (19/56, 34%) demonstrated tumour heterogeneity with more than one MI lesion phenotype (Table 4). MI tumour heterogeneity was seen in a similar proportion of TC and AC, 7/22 (32%) and 12/34 (35%), respectively. All patients in the heterogeneous group showed sites of FDG-avid disease; 11/19 (58%) patients had concordantly GaTATE positive lesions, and 8/19 (42%) had one or more discordantly GaTATE negative/FDG positive lesions (Fig. 7) rendering them MI phenotypic score 4.

Patients received PRRT

Of the 56 bronchial NET patients, 16 patients (4 TC and 12 AC) were treated with PRRT. The majority (94%) of the

Table 4 Dual-tracer analysis

Inter-patient		
MI phenotypic score	TC	AC
1 (GaTATE −ve/FDG −ve)	5/22 (23%)	1/34 (3%)
2 (GaTATE +ve/FDG −ve)	4/22 (18%)	5/34 (15%)
3 (GaTATE +ve/FDG +ve)	8/22 (36%)	11/34 (32%)
4 (GaTATE −ve/FDG +ve)	5/22 (23%)	17/34 (50%)
Intra-patient (subset of patients with more than one MI phenotype)		
1 and 3[1]	–	2/34 (6%)
1 and 4[2]	3/22 (14%)	3/34 (9%)
2 and 3[1]	3/22 (14%)	6/34 (18%)
3 and 4[2]	–	1/34 (3%)
1, 2, 3 and 4[2]	1/22 (5%)	–

MI molecular imaging, −ve negative, +ve positive

[1] Presence of intra-patient score 3 will classify the patient into the inter-patient score 3, hence potentially suitable for PRRT

[2] Presence of intra-patient score 4 will classify the patient into the inter-patient score 4, hence not suitable for PRRT

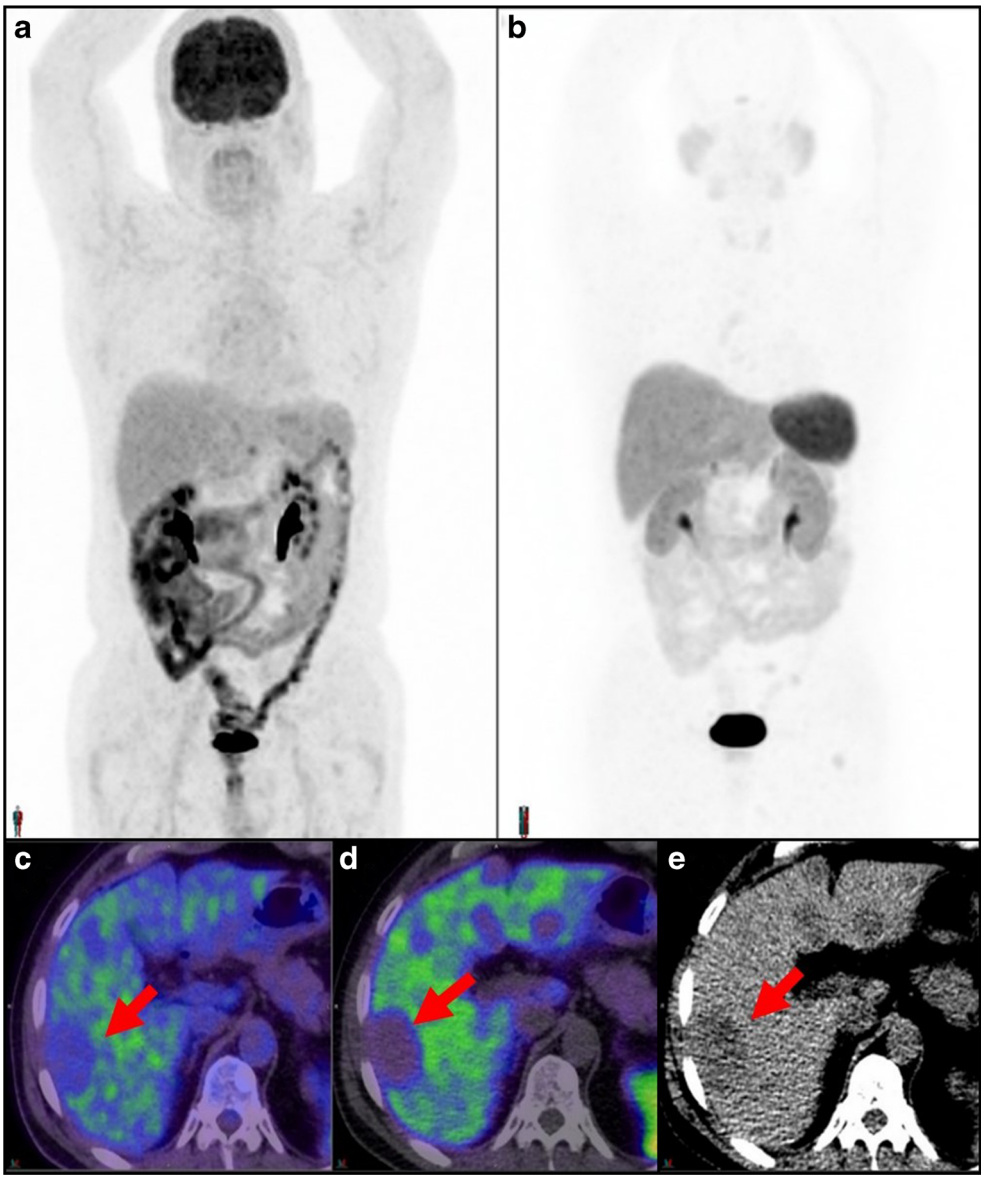

Fig. 3 Molecular imaging (MI) phenotypic score 1 in a patient with typical carcinoid. No focal lesions are identified on FDG (**a**) or GaTATE (**b**) maximum intensity projection (MIP) images, while fused FDG PET/CT (**c**), GaTATE PET/CT (**d**) and CT (**e**) show FDG negative/GaTATE negative liver lesions (arrows), which were subsequently biopsied as typical carcinoid

patients had inter-patient scores 2 and 3 (19% had score 2, and 75% had score 3). One patient had inter-patient score 4 and intra-patient scores 3 and 4 lesions. Although this patient had an unsuitable MI phenotype, based on multidisciplinary consensus, the patient was treated with PRRT for uncontrolled symptoms, despite somatostatin analogue therapy, and with the intent of palliative debulking of the large volume of GaTATE positive disease (GaTATE MITV was 1500 ml), the discordant FDG positive/GaTATE negative diseases were limited to two sites (FDG whole body MITV was 260 ml, and two sites with score 4 had MITV of 20 ml). Median time interval between dual-isotope PET scans and the first cycle of PRRT was 2.6 months (range 0.2–23 months). Most of the patients (88%) were treated due to disease progression, one patient for uncontrolled symptoms and one patient treated upfront due to the large disease burden. Fourteen patients (88%) received ^{177}Lu-DOTATATE PRRT, while 2 patients received combined/sequential ^{90}Y-DOTATATE and ^{177}Lu-DOTATATE cycles. The median cumulative activity of ^{177}Lu-DOTATATE was 31 GBq (range 6–39 GBq), with a median of 4 cycles (range 3–4). Eleven patients (69%) had also radiosensitising chemotherapy (infusional 5FU, etoposide or capecitabine with or without temozolomide).

At 3 months post-PRRT, of 14/16 patients with RECIST-measurable disease, the disease control rate (DCR) was 11/14 (79%), 43% partial response (PR) and 36% stable disease (SD). Excluding the patient with inter-patient score 4, who had PD on RECIST at 3 months post PRRT, the remaining patients with suitability for PRRT based on MI phenotype achieved a DCR of 85%, 46% PR and 39% SD. Median OS of the patients received PRRT was 54.6 months (95% CI 44–70) (Fig. 2b). The number of patients who received PRRT

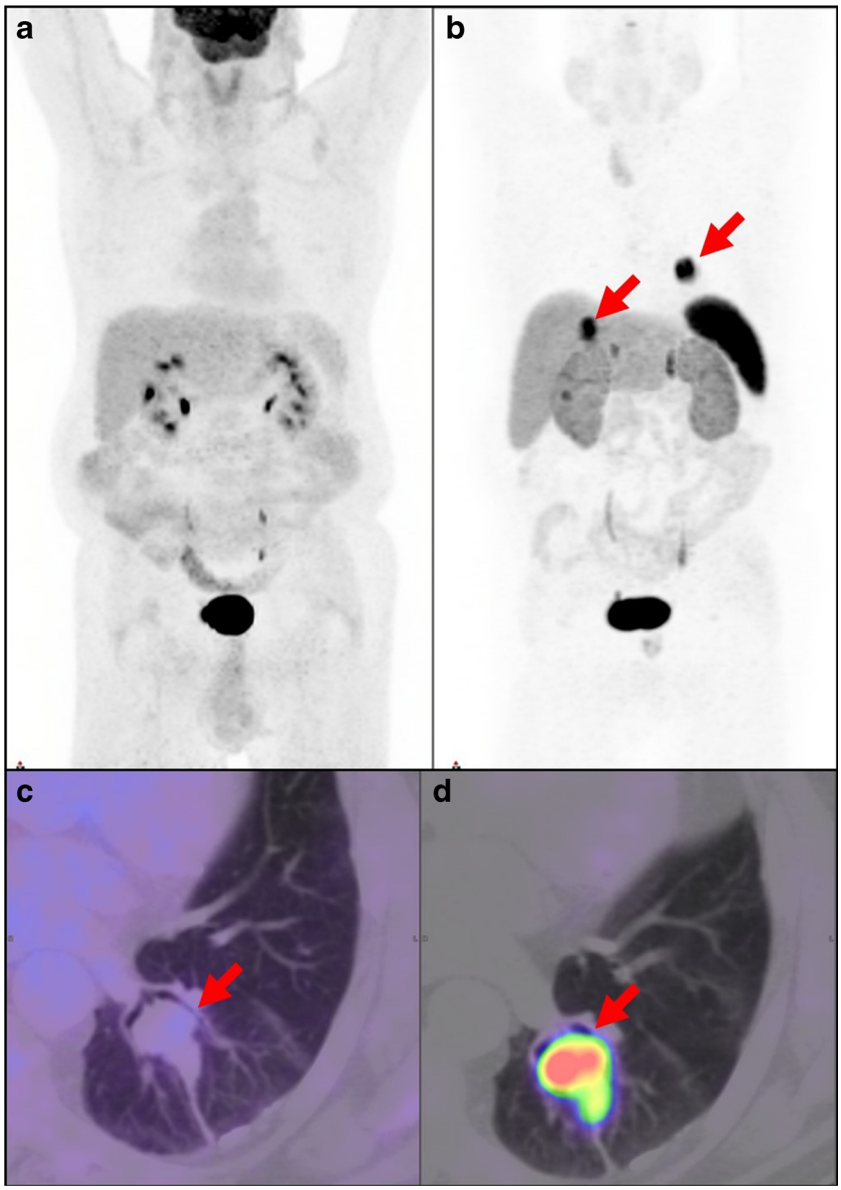

Fig. 4 Molecular imaging (MI) phenotypic score 2 in a patient with atypical carcinoid. FDG (**a**) and GaTATE (**b**) maximum intensity projection (MIP) images and fused FDG PET/CT (**c**) and GaTATE PET/CT (**d**) show FDG negative/GaTATE positive pulmonary (arrow on the MIP and fused images) and hepatic (arrow only on MIP images) lesions

with inter-patient score 2 (3 patients) was low compared with those with score 3 (12 patients), likely related to a higher likelihood of progressive disease in the latter, but OS appeared similar.

Discussion

MI using sequential GaTATE-PET and FDG-PET/CT can characterise patients with well- and poorly differentiated GEP NEN. Limited studies have reported on the detection rate of GaTATE-PET and FDG-PET/CT in the pre-operative setting in pulmonary NEN, but there is a paucity of data on its impact on the selection of patients for PRRT [32]. Furthermore, intra-patient disease heterogeneity is of clinical relevance and may explain the non-uniform therapeutic response in NET [20]. Patients who lack sufficient SSTR-ligand uptake or demonstrate spatially discordant FDG-positive/SSTR imaging negative disease are usually deemed unsuitable for PRRT. In this study, contemporaneous GaTATE-PET and FDG-PET show substantial inter- and intra-patient phenotype heterogeneity in both TC and AC groups. Almost half of the patients were unsuitable for PRRT regardless of the subtype of pulmonary NET. However, in the subgroup who had suitable dual-isotope MI phenotype (15/56 patients), following administration of PRRT a high DCR (85%) and relatively long OS (54 months) was observed. Our findings were consistent with prior studies that demonstrated DCR and OS of 60–68% and 40–52 months, respectively [33–36].

The additional value of FDG-PET to GaTATE-PET has been described previously in guiding management choice and suitability of PRRT for GEP NET patients, where FDG-

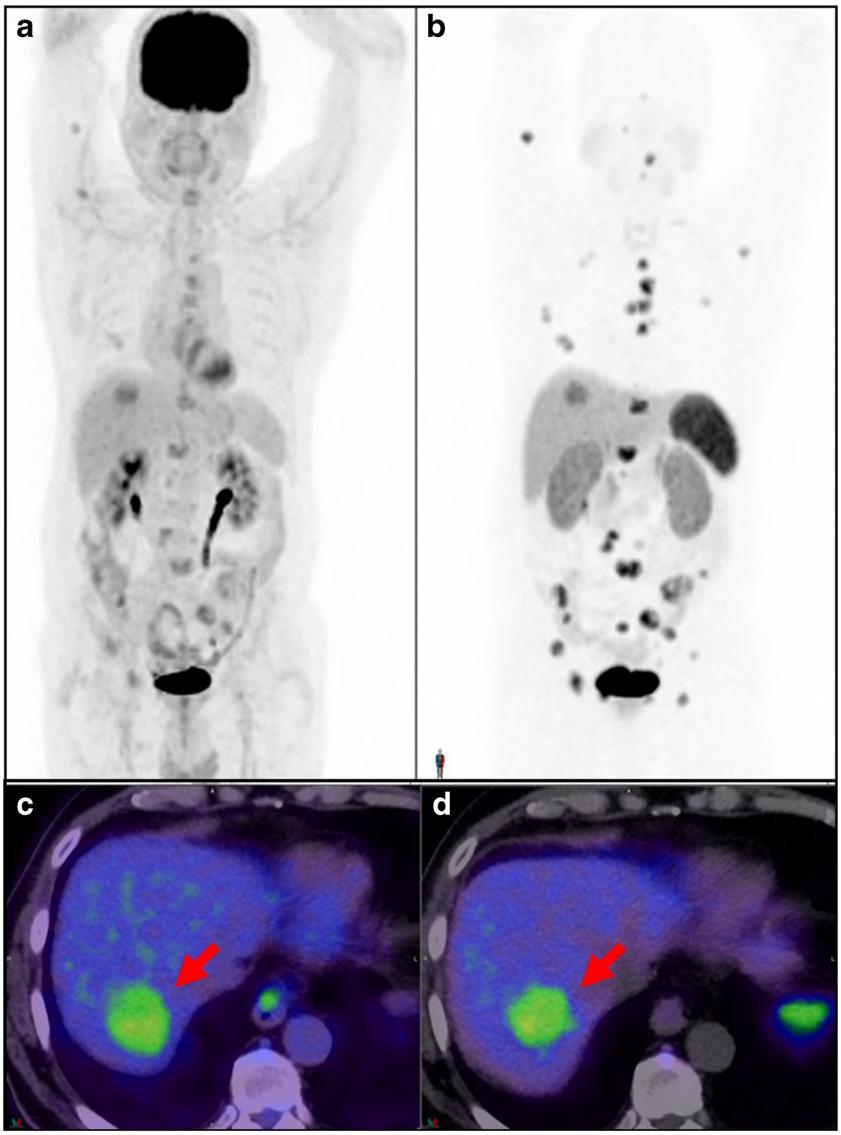

Fig. 5 Molecular imaging (MI) phenotypic score 3 in a patient with atypical carcinoid. FDG (**a**) and GaTATE (**b**) maximum intensity projection (MIP) images show concordant multifocal FDG positive/GaTATE positive liver lesions and bone lesions, with a concordant liver lesion (arrows) on fused FDG PET/CT (**c**) and GaTATE PET/CT (**d**)

PET found to play a crucial role in poorly differentiated NET but more limited impact on well-differentiated NET [37]. In a more recent study, the incremental value of FDG-PET for well-differentiated GEP NET based on Ki-67 score has been demonstrated with increased sensitivity of FDG-PET from 50 to 67% in the group with Ki67 $\geq$ 10% [38]. A limited number of studies involving patients with pulmonary NET have indicated that AC usually shows high FDG uptake and low or moderate SSTR imaging avidity, in contrast to TC, which demonstrates high SSTR imaging avidity and low or absent FDG avidity [7, 32, 39]. Consistent with prior reports, 82% of AC patients in this study had FDG positive disease, including 50% who had spatially discordant FDG-positive/GaTATE-negative disease. However, 59% of TC patients in this study were also found to have FDG-positive disease, including 23% with the spatially discordant disease. Our findings suggest that marked disease heterogeneity exists in well-differentiated pulmonary NET, highlighting the importance of dual-tracer imaging regardless of the subtype.

Our assessment included single-tracer and dual-tracer analysis that differs from the NETPET score [40] in defining the positive lesions and the grading scheme. In NETPET scoring, the background physiological uptake was used as the threshold to define positive lesions. NETPET grade uses a 6-categorical scale (P0–P5) as follows: P0, both negative; P1, SSTR-positive/FDG negative; P2–4, both positive and P5, FDG-positive/SSTR-negative. Chan et al. in a study included 62 GEP NET patients highlighted the prognostic significance of NETPET scoring system [41]. However, in this study, liver threshold was used to define positive lesions with the emphasis to guide therapeutic management in selecting the patients which may benefit from PRRT. By this simplified 4-point dual-tracer classification, we have

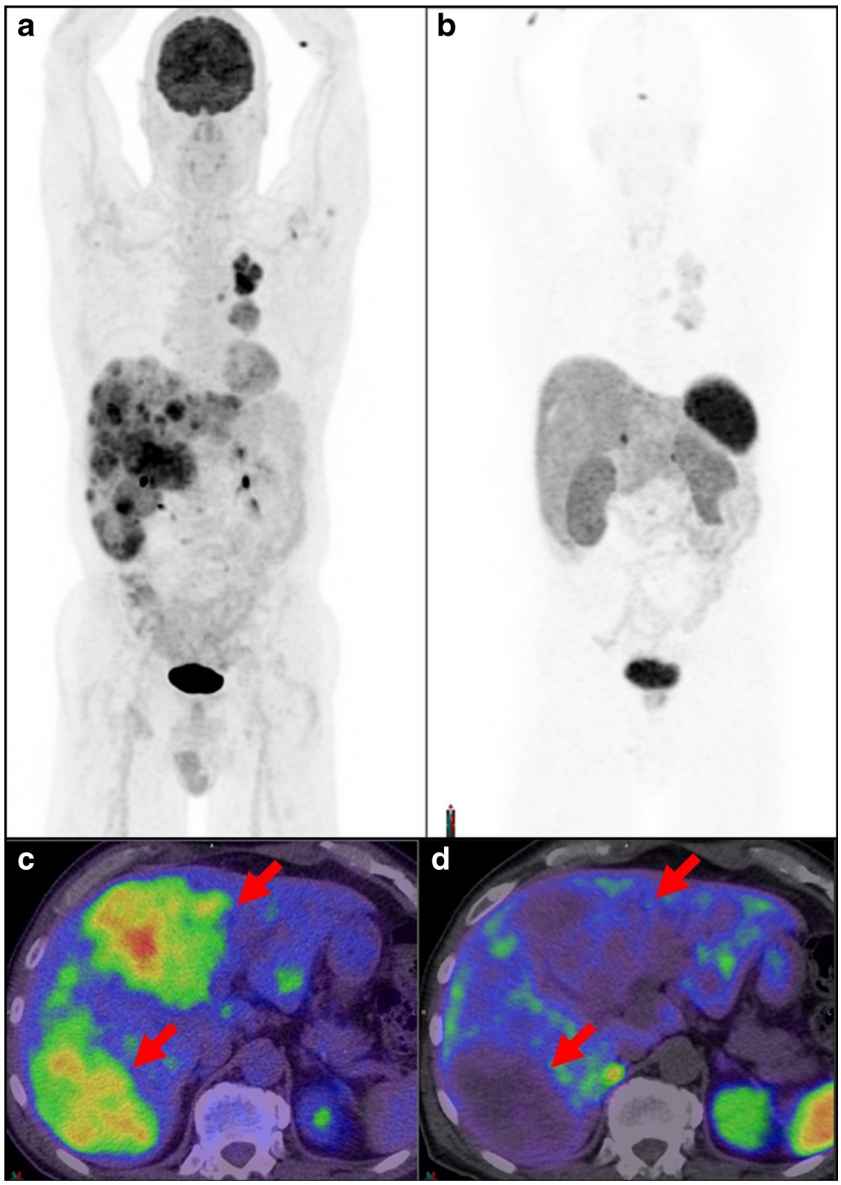

Fig. 6 Molecular imaging (MI) phenotypic score 4 in a patient with atypical carcinoid. FDG (**a**) and GaTATE (**b**) maximum intensity projection (MIP) images and fused FDG PET/CT (**c**) and GaTATE PET/CT (**d**) show multifocal FDG positive/ GaTATE negative liver lesions (arrows)

shown almost half of the patients with pulmonary NET may not be suitable for PRRT regardless of the subtype (46% in TC and 53% in AC).

Several studies showed that FDG positive disease for metastatic GEP NET predicts poor prognosis and short survival [42]. Ramirez et al. performed a study that included pulmonary NET patients. The majority of 86 patients with available FDG-PET had FDG-avid disease (85%), while of the 132 patients with SSTR imaging, almost half (53%) had positive lesions [43]. Although the head-to-head comparison between the two groups was not performed, both cohorts had similarly long OS. Our results are in general agreement with this study, with no significant stratification of the survival by FDG-avidity. In particular, patients with AC had favourable survival despite a high proportion with FDG-positive and metastatic disease. In addition, tumour volumes either on FDG-PET or GaTATE have demonstrated an inverse correlation with the patient survival in neuroendocrine tumours of the predominantly small intestine of pancreas origin [44, 45]. In this study, however, we did not find a significant correlation with the patients' survival. It should be noted a firm conclusion cannot be drawn due to a relatively low number of patients and events which has limited the statistical power of the study. Further prospective studies with a larger number of patients are required to further explore the prognostic utility of dual-tracer imaging and MI parameters in pulmonary NET.

Interestingly, there was a subset of patients with low or no GaTATE and/or FDG uptake (11%) in some or all lesions, even in the TC group. It is important, however, to consider several pitfalls prior to classifying these lesions as negative. These pitfalls include partial volume effect in small lesions at, or below, the spatial resolution of PET cameras or cystic

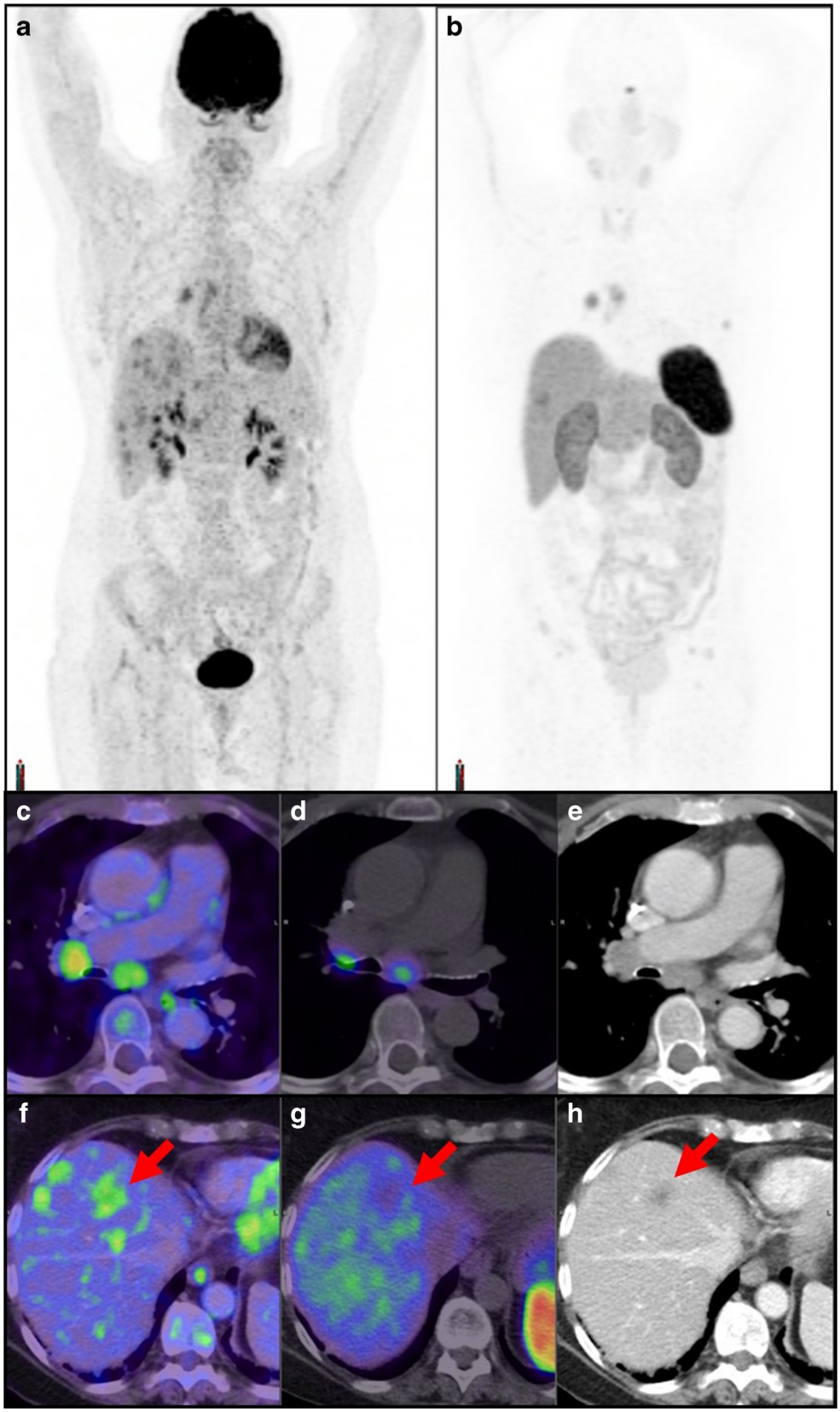

Fig. 7 Intra-patient dual-tracer heterogeneity in atypical pulmonary NET. **a** FDG and **b** GaTATE PET maximum intensity projection (MIP) images demonstrate discordant disease distribution. Fused FDG (**c**) and GaTATE PET/CT (**d**) of enlarged mediastinal nodes on CT (**e**) show score FDG positive/GaTATE positive (molecular imaging [MI] phenotypic score 3), while FDG PET/CT (**f**), GaTATE PET/CT (**g**) and CT (h) reveal FDG positive/GaTATE negative (MI phenotypic score 4) liver lesions (arrows)

lesions with a thin rind of viable tumour. We strove to select only measurable (> 1 cm) and non-cystic lesions for the purpose of this study to minimise this potential confounding factor. Variable radiotracer kinetic in different lesions may need to be considered, as the early time-point imaging of ^{68}Gallium PET tracers (45 min post-injection) may not always translate to similar intensity uptake at a more delayed time-point imaging by longer half-life tracers such as ^{111}indium or ^{177}lutetium labelled SSTR imaging. Generally, in most cases due to higher spatial resolution of PET technology, similar or higher intensity of uptake has been seen on SSTR PET imaging compared with delayed time-point imaging by ^{111}indium or ^{177}lutetium labelled SSTR imaging [46]. However, in our experience, we have rarely observed lesions with low-intensity GaTATE-PET uptake that accumulated higher intensity ^{177}Lu-DOTATATE uptake. Having considered the abovementioned factors, there appears to be a cohort of patients who have low expression of SSTR and even GLUT1. Exploring other targets than SSTR2 would be of interest to this cohort. Pulmonary NET has been reported to express other peptide receptors, including VIP (mainly VPAC1), cholecystokinin (CCK_2), Bombesin (BB_3) and GLP-1 receptors [9]. Gotthardt et al. in a study included 60 NET patients with foregut, midgut and hindgut primary has shown gastrin receptor scintigraphy (GRS) is of value in SSTR negative disease as it detected additional sites of disease in 20% of the patients [47]. Further studies in this domain would be warranted as these targets may also be used for radionuclide therapy.

One of the limitations of this study was the lack of histopathology in more than one metastatic tumour sites. Although it was not practical to biopsy multiple sites of disease in each patient, we have tried to collect the results of all available biopsies. Future studies including histological assessment based on dual-tracer MI phenotype and correlated with immunohistochemistry assessment (including GLUT1, SSTR subtypes and other emerging targets), and genomics should be considered to further enhance our understanding of this heterogeneous disease. Although the median time between the histopathological diagnosis and MI studies was 2 months, in a few patients there was a long gap (range up to 59 months). Despite the best effort to acquire new biopsy when the MI phenotype was not consistent with known tumour subtype, it remains possible that the tumour may have evolved in some of these patients during this period.

Conclusion

Pulmonary NET demonstrates a wide range of MI inter- and intra-patient heterogeneity on GaTATE and FDG-PET. Regardless of the histological type, dual-tracer imaging is important for optimal treatment selection, as almost half of the patients have sites of disease which may not be optimally targeted by PRRT. Selecting suitable patients for PRRT based on MI phenotype leads to high DCR and long OS.

Authors' contributions All authors contributed to the study concept and design. Material preparation, data collection, and analysis were performed by LZ, AI, GK, TA, MM and RJH. The first draft of the manuscript was written by LZ and AI, and all authors commented on previous versions of the manuscript. All authors read and approved the final manuscript.

Funding information This work was partly funded by the Peter Mac Foundation and supported by an NHMRC Practitioner Fellowship of the Australian Health and Medical Research Foundation to Professor Hicks (APP1108050).

Data availability The datasets generated during and/or analysed during the current study are available from the corresponding author on reasonable request.

Compliance with ethical standards

Conflict of interest The authors declare that they have no conflict of interest relevant to this paper.

Ethical approval Ethical approval was granted by the local Ethics Committee of Peter MacCallum Cancer Centre (Peter Mac Project No: 19/214R). In view of the retrospective nature of the study and all the procedures being performed were part of the routine care; the individual patient consent was waived by the Ethics Committee.

References

1. Oberg K, Hellman P, Ferolla P, Papotti M, Group EGW. Neuroendocrine bronchial and thymic tumors: ESMO Clinical Practice Guidelines for diagnosis, treatment and follow-up. Ann Oncol. 2012;23(Suppl 7):vii120–3. https://doi.org/10.1093/annonc/mds267.
2. Travis WD, Rush W, Flieder DB, Falk R, Fleming MV, Gal AA, et al. Survival analysis of 200 pulmonary neuroendocrine tumors with clarification of criteria for atypical carcinoid and its separation from typical carcinoid. Am J Surg Pathol. 1998;22:934–44. https://doi.org/10.1097/00000478-199808000-00003.
3. Travis WD. Lung tumours with neuroendocrine differentiation. Eur J Cancer. 2009;45(Suppl 1):251–66. https://doi.org/10.1016/S0959-8049(09)70040-1.
4. Travis WD, Brambilla E, Nicholson AG, Yatabe Y, Austin JHM, Beasley MB, et al. The 2015 World Health Organization classification of lung tumors: impact of genetic, clinical and radiologic advances since the 2004 classification. J Thorac Oncol. 2015;10:1243–60. https://doi.org/10.1097/JTO.0000000000000630.
5. Garg R, Bal A, Das A, Singh N, Singh H. Proliferation marker (Ki67) in sub-categorization of neuroendocrine tumours of the lung. Turk Patoloji Derg. 2019;35:15–21. https://doi.org/10.5146/tjpath.2018.01436.
6. Pelosi G, Sonzogni A, Harari S, Albini A, Bresaola E, Marchio C, et al. Classification of pulmonary neuroendocrine tumors: new insights. Transl Lung Cancer Res. 2017;6:513–29. https://doi.org/10.21037/tlcr.2017.09.04.

7. Hann CL, Forde PM. Lung and thymic carcinoids. Endocrinol Metab Clin N Am. 2018;47:699–709. https://doi.org/10.1016/j.ecl.2018.04.011.
8. Gugger M, Burckhardt E, Kappeler A, Hirsiger H, Laissue JA, Mazzucchelli L. Quantitative expansion of structural genomic alterations in the spectrum of neuroendocrine lung carcinomas. J Pathol. 2002;196:408–15. https://doi.org/10.1002/path.1065.
9. Reubi JC, Waser B. Concomitant expression of several peptide receptors in neuroendocrine tumours: molecular basis for in vivo multireceptor tumour targeting. Eur J Nucl Med Mol Imaging. 2003;30:781–93. https://doi.org/10.1007/s00259-003-1184-3.
10. Melosky B. Advanced typical and atypical carcinoid tumours of the lung: management recommendations. Curr Oncol. 2018;25:S86–93. https://doi.org/10.3747/co.25.3808.
11. Pusceddu S, Lo Russo G, Macerelli M, Proto C, Vitali M, Signorelli D, et al. Diagnosis and management of typical and atypical lung carcinoids. Crit Rev Oncol Hematol. 2016;100:167–76. https://doi.org/10.1016/j.critrevonc.2016.02.009.
12. Kabasakal L, Demirci E, Ocak M, Decristoforo C, Araman A, Ozsoy Y, et al. Comparison of (6)(8)Ga-DOTATATE and (6)(8)Ga-DOTANOC PET/CT imaging in the same patient group with neuroendocrine tumours. Eur J Nucl Med Mol Imaging. 2012;39:1271–7. https://doi.org/10.1007/s00259-012-2123-y.
13. Velikyan I, Sundin A, Sorensen J, Lubberink M, Sandstrom M, Garske-Roman U, et al. Quantitative and qualitative intrapatient comparison of 68Ga-DOTATOC and 68Ga-DOTATATE: net uptake rate for accurate quantification. Journal of nuclear medicine : official publication, Society of Nuclear Medicine. 2014;55:204–10. https://doi.org/10.2967/jnumed.113.126177.
14. Hofman MS, Kong G, Neels OC, Eu P, Hong E, Hicks RJ. High management impact of Ga-68 DOTATATE (GaTate) PET/CT for imaging neuroendocrine and other somatostatin expressing tumours. J Med Imaging Radiat Oncol. 2012;56:40–7. https://doi.org/10.1111/j.1754-9485.2011.02327.x.
15. Hicks RJ. Use of molecular targeted agents for the diagnosis, staging and therapy of neuroendocrine malignancy. Cancer Imaging. 2010;10 Spec no A:S83–91. doi:https://doi.org/10.1102/1470-7330.2010.9007.
16. Lococo F, Treglia G, Cesario A, Paci M, Filice A, Versari A, et al. Functional imaging evaluation in the detection, diagnosis, and histologic differentiation of pulmonary neuroendocrine tumors. Thorac Surg Clin. 2014;24:285–92. https://doi.org/10.1016/j.thorsurg.2014.04.004.
17. Treglia G, Giovanella L, Lococo F. Evolving role of PET/CT with different tracers in the evaluation of pulmonary neuroendocrine tumours. Eur J Nucl Med Mol Imaging. 2014;41:853–5. https://doi.org/10.1007/s00259-014-2695-9.
18. Hofman MS, Lau WF, Hicks RJ. Somatostatin receptor imaging with 68Ga DOTATATE PET/CT: clinical utility, normal patterns, pearls, and pitfalls in interpretation. Radiographics : a review publication of the Radiological Society of North America, Inc. 2015;35:500–16. https://doi.org/10.1148/rg.352140164.
19. Van Essen M, Krenning EP, De Jong M, Valkema R, Kwekkeboom DJ. Peptide receptor radionuclide therapy with radiolabelled somatostatin analogues in patients with somatostatin receptor positive tumours. Acta Oncol. 2007;46:723–34. https://doi.org/10.1080/02841860701441848.
20. Hofman MS, Hicks RJ. Changing paradigms with molecular imaging of neuroendocrine tumors. Discov Med. 2012;14:71–81.
21. Werner RA, Weich A, Kircher M, Solnes LB, Javadi MS, Higuchi T, et al. The theranostic promise for neuroendocrine tumors in the late 2010s - where do we stand, where do we go? Theranostics. 2018;8:6088–100. https://doi.org/10.7150/thno.30357.
22. Hofman MS, Hicks RJ. Peptide receptor radionuclide therapy for neuroendocrine tumours: standardized and randomized, or personalized? Eur J Nucl Med Mol Imaging. 2014;41:211–3. https://doi.org/10.1007/s00259-013-2621-6.
23. Kong G, Grozinsky-Glasberg S, Hofman MS, Akhurst T, Meirovitz A, Maimon O, et al. Highly favourable outcomes with peptide receptor radionuclide therapy (PRRT) for metastatic rectal neuroendocrine neoplasia (NEN). Eur J Nucl Med Mol Imaging. 2019;46:718–27. https://doi.org/10.1007/s00259-018-4196-8.
24. Carideo L, Prosperi D, Panzuto F, Magi L, Pratesi MS, Rinzivillo M, et al. Role of combined [(68)Ga]Ga-DOTA-SST analogues and [(18)F]FDG PET/CT in the management of GEP-NENs: a systematic review. J Clin Med. 2019;8. https://doi.org/10.3390/jcm8071032.
25. Pattison DA, MacFarlane LL, Callahan J, Kane EL, Akhurst T, Hicks RJ. Personalised insulin calculator enables safe and effective correction of hyperglycaemia prior to FDG PET/CT. EJNMMI Res. 2019;9:15. https://doi.org/10.1186/s13550-019-0480-2.
26. Barrington SF, Mikhaeel NG, Kostakoglu L, Meignan M, Hutchings M, Mueller SP, et al. Role of imaging in the staging and response assessment of lymphoma: consensus of the international conference on malignant lymphomas imaging working group. Journal of clinical oncology : official journal of the American Society of Clinical Oncology. 2014;32:3048–58. https://doi.org/10.1200/JCO.2013.53.5229.
27. Kong G, Callahan J, Hofman MS, Pattison DA, Akhurst T, Michael M, et al. High clinical and morphologic response using (90)Y-DOTA-octreotate sequenced with (177)Lu-DOTA-octreotate induction peptide receptor chemoradionuclide therapy (PRCRT) for bulky neuroendocrine tumours. Eur J Nucl Med Mol Imaging. 2017;44:476–89. https://doi.org/10.1007/s00259-016-3527-x.
28. Hubble D, Kong G, Michael M, Johnson V, Ramdave S, Hicks RJ. 177Lu-octreotate, alone or with radiosensitising chemotherapy, is safe in neuroendocrine tumour patients previously treated with high-activity 111In-octreotide. Eur J Nucl Med Mol Imaging. 2010;37:1869–75. https://doi.org/10.1007/s00259-010-1483-4.
29. Hicks RJ, Kwekkeboom DJ, Krenning E, Bodei L, Grozinsky-Glasberg S, Arnold R, et al. ENETS consensus guidelines for the standards of care in neuroendocrine neoplasia: peptide receptor radionuclide therapy with radiolabeled somatostatin analogues. Neuroendocrinology. 2017;105:295–309. https://doi.org/10.1159/000475526.
30. Kong G, Johnston V, Ramdave S, Lau E, Rischin D, Hicks RJ. High-administered activity in-111 octreotide therapy with concomitant radiosensitizing 5FU chemotherapy for treatment of neuroendocrine tumors: preliminary experience. Cancer Biother Radiopharm. 2009;24:527–33. https://doi.org/10.1089/cbr.2009.0644.
31. Eisenhauer EA, Therasse P, Bogaerts J, Schwartz LH, Sargent D, Ford R, et al. New response evaluation criteria in solid tumours: revised RECIST guideline (version 1.1). Eur J Cancer. 2009;45:228–47. https://doi.org/10.1016/j.ejca.2008.10.026.
32. Lococo F, Perotti G, Cardillo G, De Waure C, Filice A, Graziano P, et al. Multicenter comparison of 18F-FDG and 68Ga-DOTA-peptide PET/CT for pulmonary carcinoid. Clin Nucl Med. 2015;40:e183–9. https://doi.org/10.1097/RLU.0000000000000641.
33. Ianniello A, Sansovini M, Severi S, Nicolini S, Grana CM, Massri K, et al. Peptide receptor radionuclide therapy with (177)Lu-DOTATATE in advanced bronchial carcinoids: prognostic role of thyroid transcription factor 1 and (18)F-FDG PET. Eur J Nucl Med Mol Imaging. 2016;43:1040–6. https://doi.org/10.1007/s00259-015-3262-8.
34. Sabet A, Haug AR, Eiden C, Auernhammer CJ, Simon B, Bartenstein P, et al. Efficacy of peptide receptor radionuclide therapy with (177)Lu-octreotate in metastatic pulmonary neuroendocrine tumors: a dual-centre analysis. American journal of nuclear medicine and molecular imaging. 2017;7:74–83.

35. Parghane RV, Talole S, Prabhash K, Basu S. Clinical response profile of metastatic/advanced pulmonary neuroendocrine tumors to peptide receptor radionuclide therapy with 177Lu-DOTATATE. Clin Nucl Med. 2017;42:428–35. https://doi.org/10.1097/RLU.0000000000001639.
36. Brabander T, van der Zwan WA, Teunissen JJM, Kam BLR, Feelders RA, de Herder WW, et al. Long-term efficacy, survival, and safety of [(177)Lu-DOTA(0),Tyr(3)]octreotate in patients with gastroenteropancreatic and bronchial neuroendocrine tumors. Clinical cancer research : an official journal of the American Association for Cancer Research. 2017;23:4617–24. https://doi.org/10.1158/1078-0432.CCR-16-2743.
37. Panagiotidis E, Alshammari A, Michopoulou S, Skoura E, Naik K, Maragkoudakis E, et al. Comparison of the impact of 68Ga-DOTATATE and 18F-FDG PET/CT on clinical management in patients with neuroendocrine tumors. J Nucl Med. 2017;58:91–6. https://doi.org/10.2967/jnumed.116.178095.
38. Zhang P, Yu J, Li J, Shen L, Li N, Zhu H, et al. Clinical and prognostic value of PET/CT imaging with combination of (68)Ga-DOTATATE and (18)F-FDG in gastroenteropancreatic neuroendocrine neoplasms. Contrast Media Mol Imaging. 2018;2018:2340389. https://doi.org/10.1155/2018/2340389.
39. Jiang Y, Hou G, Cheng W. The utility of 18F-FDG and 68Ga-DOTA-Peptide PET/CT in the evaluation of primary pulmonary carcinoid: a systematic review and meta-analysis. Medicine (Baltimore). 2019;98:e14769. https://doi.org/10.1097/MD.0000000000014769.
40. Hindie E. The NETPET score: combining FDG and somatostatin receptor imaging for optimal management of patients with metastatic well-differentiated neuroendocrine tumors. Theranostics. 2017;7:1159–63. https://doi.org/10.7150/thno.19588.
41. Chan DL, Pavlakis N, Schembri GP, Bernard EJ, Hsiao E, Hayes A, et al. Dual somatostatin receptor/FDG PET/CT imaging in metastatic neuroendocrine tumours: proposal for a novel grading scheme with prognostic significance. Theranostics. 2017;7:1149–58. https://doi.org/10.7150/thno.18068.
42. Bahri H, Laurence L, Edeline J, Leghzali H, Devillers A, Raoul JL, et al. High prognostic value of 18F-FDG PET for metastatic gastroenteropancreatic neuroendocrine tumors: a long-term evaluation. J Nucl Med. 2014;55:1786–90. https://doi.org/10.2967/jnumed.114.144386.
43. Ramirez RA, Beyer DT, Diebold AE, Voros BA, Chester MM, Wang YZ, et al. Prognostic factors in typical and atypical pulmonary carcinoids. Ochsner J. 2017;17:335–40.
44. Chan DL, Bernard E, Schembri G, Roach P, Johnson M, Pavlakis N, et al. High metabolic tumour volume on FDG PET predicts poor survival from neuroendocrine neoplasms. Neuroendocrinology. 2019. https://doi.org/10.1159/000504673.
45. Tirosh A, Papadakis GZ, Millo C, Hammoud D, Sadowski SM, Herscovitch P, et al. Prognostic utility of total (68)Ga-DOTATATE-avid tumor volume in patients with neuroendocrine tumors. Gastroenterology. 2018;154:998–1008 **e1**. https://doi.org/10.1053/j.gastro.2017.11.008.
46. Hope TA, Calais J, Zhang L, Dieckmann W, Millo C. (111)In-pentetreotide scintigraphy versus (68)Ga-DOTATATE PET: impact on Krenning scores and effect of tumor burden. J Nucl Med. 2019;60:1266–9. https://doi.org/10.2967/jnumed.118.223016.
47. Gotthardt M, Behe MP, Grass J, Bauhofer A, Rinke A, Schipper ML, et al. Added value of gastrin receptor scintigraphy in comparison to somatostatin receptor scintigraphy in patients with carcinoids and other neuroendocrine tumours. Endocr Relat Cancer. 2006;13:1203–11. https://doi.org/10.1677/erc.1.01245.